Research Article   OMICS International

Surface Dose Assessment for Different Clinical set up Parameters from High Energy Photon Beams

Attalla EM[1,2*], El-Sayed AA[3], Hessein H[3], Abouelenein HS[1] and Ashour EF[4]

[1]Children's Cancer Hospital, Egypt

[2]National Cancer Institute, Cairo University, Egypt

[3]Biophysics Department, Faculty of Science, Cairo University, Egypt

[4]El-Sweedy Oncology Center, Egypt

*Corresponding author: Ehab M Attalla, National Cancer Institute, Cairo University, Egypt, Tel: 20 120 828 5664, E-mail: attalla.ehab@gmail.com

Abstract

Introduction: The purpose of this study was to investigate surface doses of 6 and 10 MV energies of linear accelerator for different clinical setup parameters including (field size, gantry angle, SSD (source skin distance), PW (physical wedge), acrylic block tray and bolus), Comparison between measured surface dose by P.P (parallel plate) and calculated surface dose by TPS (Treatment Planning system). Comparison between surface doses measured by TLD (Thermo luminescence dosimeter) and P.P ion chamber, Comparison between the surface dose of 3DCRT and IMRT techniques.

Materials and Methods: Surface dose measurements were carried out using a (PTW) Markus parallel-plate ion chamber in a plastic water plastic water phantom for various setup parameters using Primus Siemens (6, 10 MV) linear accelerator. For the normalization depth, i.e., the depth of maximum dose 1.5, 2.5 cm were chosen for 6, 10 MV photon beams, respectively.

Results and Discussion: The measured skin dose values for 10 MV were lower than those of 6 MV, the skin dose increased as field size increased. The measured surface dose by P.P for 6 and 10 MV are 16%, 25%, for 10 × 10 cm^2 square field size, within the first 2 millimetres of the build-up region, at field size 10 × 10 cm^2 the PDD for a 6 and 10 MV photon beam increases from 24% to 62%, 16% to 44% respectively. With increasing the gantry angles (0 to 30) produces a minimal effect of dose, (40-70) gantry angles produce a significant increase. When studying the surface dose with different SSD found that the percentage of surface dose is nearly stable, the absolute surface dose (cGy) increased with decreasing SSD. The absolute skin dose for wedge fields were lower than for open fields, for field size 10 × 10 cm^2, while the values of surface dose of wedge 30 are 20% and 14% for 6 and 10 MV respectively. The skin dose for a wedge field increased as field size increased. Bolus 1 cm material increased the surface dose for 10 × 10 cm^2 from 24% to 96%, and from 16% to 87%, for 6 and 10 MV respectively. With the use of an acrylic block tray, the surface dose increased to the open fields for all field sizes higher than 10 cm^2, but the increase was dominant for large fields, for field size 20 × 20 cm^2 the surface dose increased from 29% to 41%, from 22% to 34% for 6 and 10 MV respectively.

Conclusion: Agreement between skin doses calculated by multidata TPS and those measured by P.P ion chamber in water plastic water phantom was better than 20% for 96% of measurement points and this is indicate that the dose calculation in the build-up region using multidata TPS is good. For irregular tumor shape and closed OAR the IMRT is a good solution to cover the tumor and spare the critical organs without increasing the skin dose.

Keywords: Surface dose; Parallel plate ionization chamber; TLD; IMRT; Dose calculation

Introduction

Skin dose has two components depending on secondary electrons produced from photon interactions with air, collimator jaws, the patient surface and any other scattering material. There are two steps for photon interactions, namely primary interaction and multiple scattering within the medium. There are two sources for contamination: (i) treatment head materials (collimator jaws, flattening filter, beam monitor chambers and the target) (ii) treatment setup parameters (field size, wedge, tray, block and SSD). The amounts of these contamination electrons affect the surface dose. It is not possible to change the effect of treatment head materials on skin dose in clinical applications, but skin dose can be changed by using different treatment setup parameters. Therefore, the knowledge of how parameters affect the skin dose at the skin surface is essential for proper treatment [1].

The surface dose by definition is difficult to measure; the effective point of measurement of most commonly used dosimeters ranges from several micrometers of water equivalent thickness to a few millimeters [2]. According to the ICRP and the ICRU, the skin depth recommended for practical dose assessments is at 0.07 cm and this depth generally corresponds to the interface between the epidermis and dermis layers of the skin [3-6]. The skin-sparing effect for high-

energy and X-ray photons may be reduced or even lost, if the beam is contaminated with electrons and/or low-energy photons. Since the skin dose in treatment of deep-seated tumors may be the limiting factor in the delivery of high tumor doses, the dose distribution in the build-up region should be known. The relevant dose at specification depth depends on the biological effect considered. The skin consists of three layers: the epidermis, the dermis and the subcutaneous fatty tissue. The thickness of the epidermis and dermis is 0.05-0.15 mm and 1-2 mm in most locations, respectively. The subcutaneous fatty tissues lie under the dermis. It is important to know the dose distribution of these layers before treatment because of possible biological complications of high skin doses in radiotherapy treatment, such as desquamation, erythema, fibrosis, necrosis and epilation.

The purpose of this study was to investigate surface doses of different clinical setup parameters including field size, PW, acrylic block tray, bolus, gantry angle variation and SSD for high energy photon beams.

Materials and Methods

Surface dose measurements were carried out using a (PTW) Markus parallel-plate ion chamber in a plastic water plastic water phantom for various setup parameters. The measurements were performed using Siemens primus (6 MV, 10 MV) linear accelerators at the normalization depth, the depth of maximum dose (dmax). The depth of maximum dose for 6 and 10 MV were 1.5 cm and 2.5 cm respectively.

Central axis depth dose measurements were made in a plastic water phantom using parallel-plate ion chamber. The Markus-type chamber was imbedded in a plastic water phantom and 15 cm of backscatter thickness was used to ensure plastic water phantom scatter equilibrium. Plastic water plastic water phantom sheets of 2 mm thickness were placed, on the chamber surface to measure the surface dose at 2 mm depth. A SSD of 100 cm was chosen for measurements. The absolute surface dose and the percentage surface dose at 0 and 2 mm depth were measured for each setup.

Readings at the plastic water phantom surface (depth=0) were normalized to readings at the maximum depth to obtain relative skin doses at the surface for all energies. Measurements of skin doses were performed at 100 cm SSD with different sizes of open fields ranging from 5×5 cm^2 to 40×40 cm^2. The effect of gantry angle was studied for gantry angles ranged from 0 to 70 degree. The effect of SSD was studied for different SSDs ranged from 85 cm to 120 cm. Skin dose values were obtained for 15º, 30º, 45º and 60º PW. Acrylic block tray was placed in the direction of the radiation beam to determine its effect on the skin dose. The tray was used to support the cerrobend blocks and it was placed at the accessory tray holder. 1 cm bolus material was placed on the surface of the plastic water phantom to determine its effect on the skin dose.

Treatment planning at different sites

Comparison between the surface dose for 3-DCRT and IMRT techniques were done. Three treatment plans were calculated for each site by 3-DCRT and recalculated by IMRT. For brain the tumor was drown above the brain stem and two other region were drown around the tumor as an organ at risk (OAR) to make the calculation complicated and so increase the number of segments and monitor units. For abdomen the tumor was drown above the spinal cord and between the two kidneys to simulate the neuroplastoma cases. The

third position selected at the pelvis and the tumor was drawing to simulate the prostate cases. The treatment plans were performed to deliver 200 cGy per fraction to the planning target volume (PTV). Comparison between the measured and the calculated surface dose by TPS were done.

TLD preparation

The TLDs used in this study were selected from a batch of LiF (Mg, Cu, P) circular chip having dimensions of 4.5 mm diameter and 0.8 mm thickness.

Since TLDs, as dosimeters, can be reused for hundreds of times, annealing treatment should be done prior to each irradiation. This is required especially in medical therapy applications, where high doses are the norm and the highest accuracy is desired. In the present study, LiF (Mg,Cu,P) TLDs were annealed for 10 minutes at 240°C to remove the residual charges in the competitors thereby avoiding sensitization, followed by rapid cooling according to manufacture manual.

The TLD oven was used to anneal the TLDs and a TLD reader type Fimel PCL3 (FIMEL, France) was used as the TLD reader. Pre-Heating temperature were seted from 30°C up to 400°C by 1°C steps. It must be high enough to ensure elimination of unstable beaks, while leaving dosimeter peaks intact. The heating temperature seted from 30°C up to 600°C by 1°C steps were chosen so that dosimetry peaks can be read, and always higher than pre-heating temperature. The TLDs were selected for the sensitivity within 5%.

For the TLDs calibration the Ionization Chamber used was Farmer 0.6 cc (PTW, Germany). The Plastic water phantom of dimensions 30 cm × 30 cm × 15 cm was used for the TLD calibration at depth of maximum dose dmax of the used energy which is 16 mm for the 6MV. For calibration purposes, a wide range of doses from 1 m Gy to 10 Gy were delivered from the 6 MV photon beams in the presence of the ionization chamber at the dmax and for field size 10 cm × 10 cm and source to surface distance (SSD) 100 cm. 20 sets of the used TLD batch each set contains 3 TLD chips were exposed for the same doses at the same setup conditions to obtain the TLD calibration curve. The TLD calibration curve is a relation between the TLD light signals and the TLD absorbed dose. Where we compare between two treatment techniques and we use the same number and directions of the treatment fields there was no need for special correction factors for TLD as field size, angle, wedge, dose rate dependence.

A few TLDs were separated into subgroups, which were used to test the calibration curve accuracy. These subgroups were irradiated to known doses after the establishment of the calibration curve and the TLD doses were calculated using the THD signals and the TLD calibration factor. The accuracy of TLD measurements were tested depends on the reproducibility of the result as measured by the standard deviation of each individual calibration factor. The individual backgrounds for each TLD were not subtracted from the gross readings since the background was so low compared with the TL of 100 cGy (less than 0.01% for LiF (Mg,Cu,P) circular chip.

Results and Discussion

Field size effect

Figure 1 showed the surface dose values for open fields. Skin dose increased with field size increased. Measured skin dose values for 6

MV were lower than those of 10 MV. This increase is due to increased electron emission from the collimator and air.

The results showed that within the first 2 millimeters of the build-up region, at field size 10×10 cm^2 the PDD increased from 24% to 62% for 6 MV and from 16% to 44% for 10 MV.
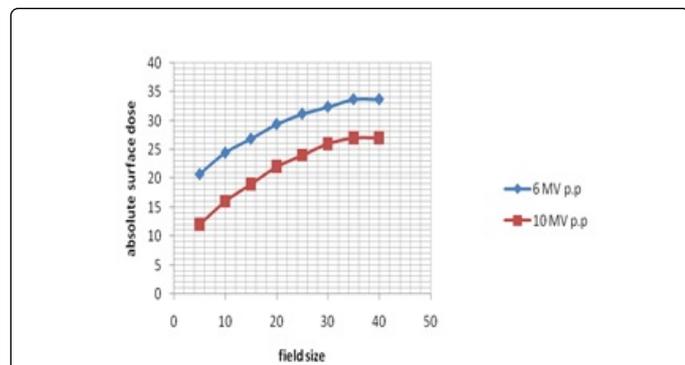

Figure 1: Absolute surface dose measured by (P.P) with different field sizes for 6 and 10 MV and SSD at surface.

Oblique incidence effect

For oblique incidence of the radiation beams with the plastic water phantom surfaces the results showed that for gantry angles from 0 to 300 there is a minimal increase in the surface dose. For gantry angles from 400 to 700 there is a significant increase in surface dose where the depth of dose maximum (dmax) is shifted toward the shallower depth. The results of skin dose measurement for gantry angle are presented in Figures 2 and 3.

From Figure 2 there was good agreement between calculated and surface dose measured with TLD and this is due to the TLD thickness which means that the surface dose was over estimated by around 15% than that measured by parallel plate ionization chamber.

From Figure 3 the results showed that for the isocentric point the surface dose increased by around 12% with oblique incidence from 0 to 600 degree of gantry angles.
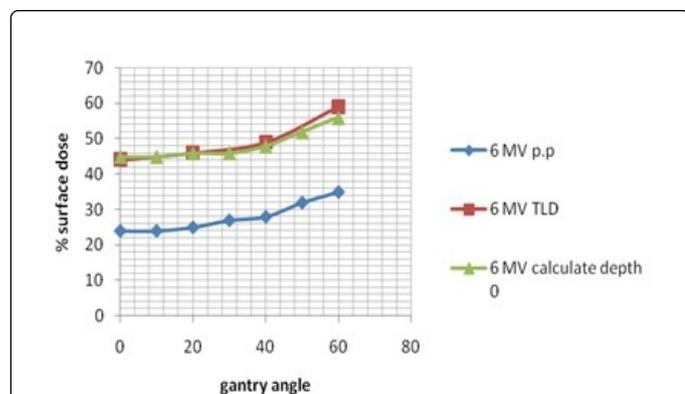

Figure 2: Comparison between the measured percentage surface dose by (TLD and P.P) and calculated by TPS with different gantry angles for 6 MV at the surface.
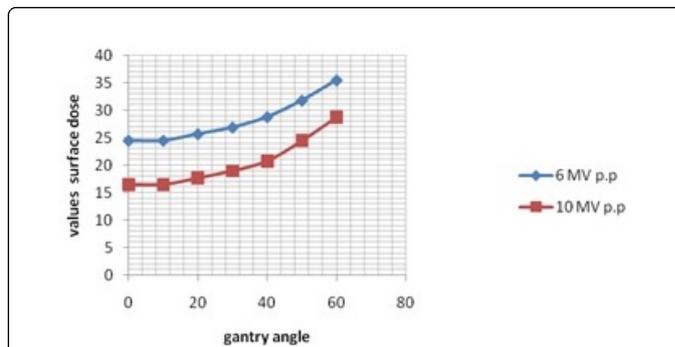

Figure 3: Absolute values of surface dose of (100 cGy /100 MU) for 6 and 10 MV.

Source skin distance effect

The results of different SSD showed that the absolute surface dose (cGy) decreased with increasing source skin distances. This increase in surface dose is due to the decreasing in the number of the low energy photons which reach the plastic water phantom surface with increasing the SSD. This beam hardening leads to shifting the dmax and so percentage depth dose toward the deeper depth. This shifting of the percentage depth dose was cleared in Figure 4 where the percentage surface dose is nearly stable with different SSD, Figures 4 and 5 and this results were agree with Girigesh et al. [7].
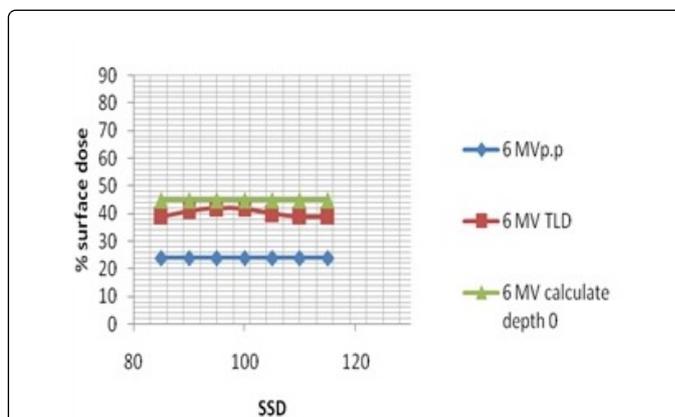

Figure 4: comparison between the measured surface dose by TLD and p. p and calculated surface dose by TPS with different SSD for 6 MV.

Physical wedge effect

The results showed that the absolute skin dose for wedge fields were lower than for open fields and this is in agreement with Bilage et al. [8]. The surface dose was decreased with increasing the wedge angle except in wedge 60; its value of surface dose is larger than that of wedge 45. For field size 10×10 cm^2, 6 MV the values of surface dose of wedge 15, 30, 45, 60 were 14.7, 10.4, 5.5 and 6.7 respectively. For 10 MV, the values of surface dose for wedge angles 15, 30, 45, 60 were 10.4, 7.9, 5 and 5.5 respectively for field size 10×10 cm^2, 10 MV. As in open fields the skin dose for the wedged fields are increased as field size increased

Figures 6 and 7. According to Kim et al. both eliminates electrons from upstream and generates electrons itself [9]. They noted that the number of electrons produced in the wedge is less than the number of electrons eliminated by the wedge for smaller field sizes and smaller wedge angles. Also the presence of the physical wedge absorbs the low energy photons and so makes beam hardening.
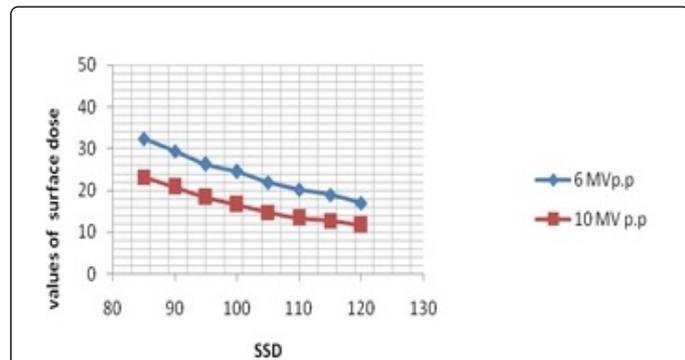

Figure 5: The measured values of surface dose by parallel plate ion chamber with different SSD for 6 MV and 10 MV at the surface.
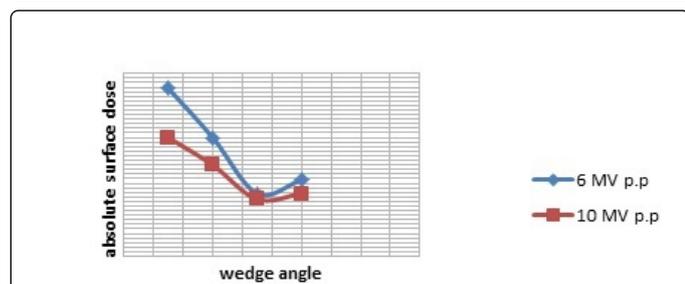

Figure 6: The measured values of surface dose by parallel plate ion chamber for different wedge angles for 6 MV and 10 MV at the surface.
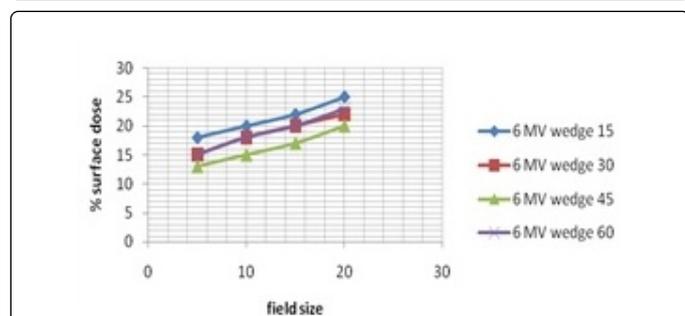

Figure 7: Comparison between the measured surface dose for wedges (15, 30, 45, 60) with different field sizes for 6 MV.

Bolus material effect

1 cm bolus material was placed on the surface of the plastic water phantom to determine its effect on the skin dose. This study found that

the percentage skin doses for open fields were lower than the percentage skin doses when adding bolus and the skin dose increased with increasing the field size. For 6 and 10 MV, the field sizes were 5 × 5, 10 × 10, 15 × 15, 20 × 20, 25 × 25 and 30 × 30 cm^2. Figure 8 showed the surface doses for 6 MV with and without bolus.
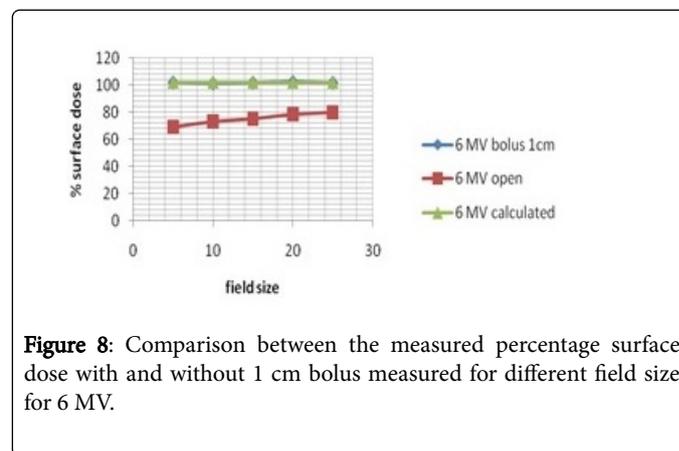

Figure 8: Comparison between the measured percentage surface dose with and without 1 cm bolus measured for different field size for 6 MV.

Block tray effect

Acrylic block tray was placed on the beam to determine its effect on the skin dose. The tray was used to support the cerrobend blocks and it was placed at the accessory tray holder. With the use of an acrylic block tray, the percentage surface dose and also the values of the surface dose are increased for all field sizes, but the increase was dominant for large fields, Figure 9 showed the surface doses for 6 MV. For 10 MV, with field sizes 10, 20, 30 and 40 cm^2 the surface dose at open fields were 16%, 22%, 26% and 27% and with tray the values increased to 18%, 34%, 50% and 62% respectively. These results are agreed with Nadir et al [1].
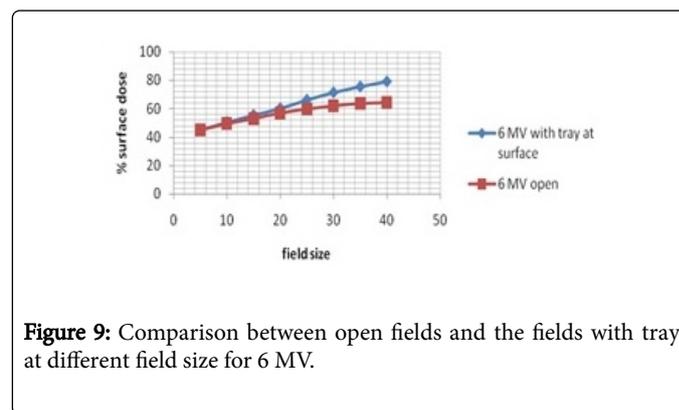

Figure 9: Comparison between open fields and the fields with tray at different field size for 6 MV.

The impact of clinical treatment planning setup on surface doses

To compare between surface dose in three dimension conformal radiotherapy (3DCRT) and intensity modulated radiotherapy (IMRT) three treatment plans were made for three treatment sites (brain, abdomen and pelvic).

Surface doses were calculated at 3D treatment planning system of Xio, using superposition calculation algorism and compared with the measurements using TLD. Three treatment plans of five fields for three different sites, Brain, Abdomen and Pelvic were prepared to deliver 100

cGy for the Brain, Abdomen and Pelvic target volume. For the two treatment techniques 3DCRT and IMRT, the plans were calculated to deliver the same dose with the same gantry angles 0º, 72º, 144º, 216º and 288º.

Figure 10 showed beam shape with Multi leaf collimator in brain case that conform as closely as possible to the target volume. Figure 11 showed the same traditional beam but in IMRT where the radiation beam splitted into many segments with different intensities to make Intensity map. The dark squares referred to high dose regions and white squares had low doses. The main differences bet 3DCRT and IMRT were showed in Figure 10 and 11 where in 3DCRT the radiation beam had the same intensity even though there were critical organs in the open beam but as shown in Figure 11 using IMRT the dose for critical organ can be decreased by decreasing the beam intensity from this segment.
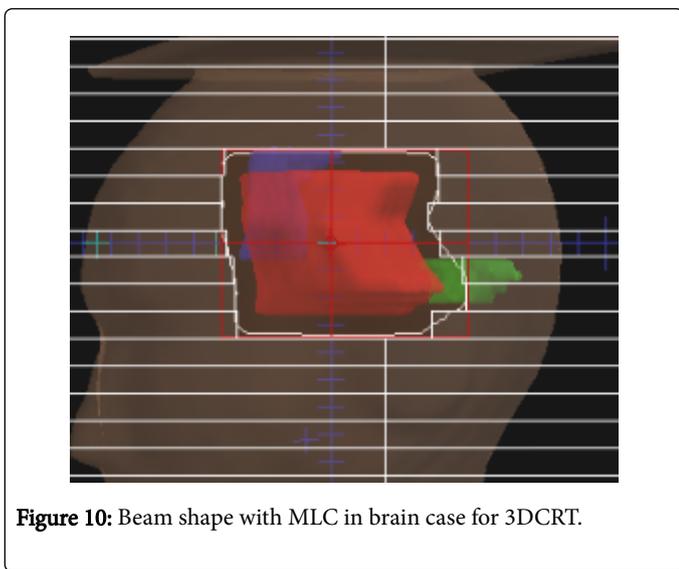

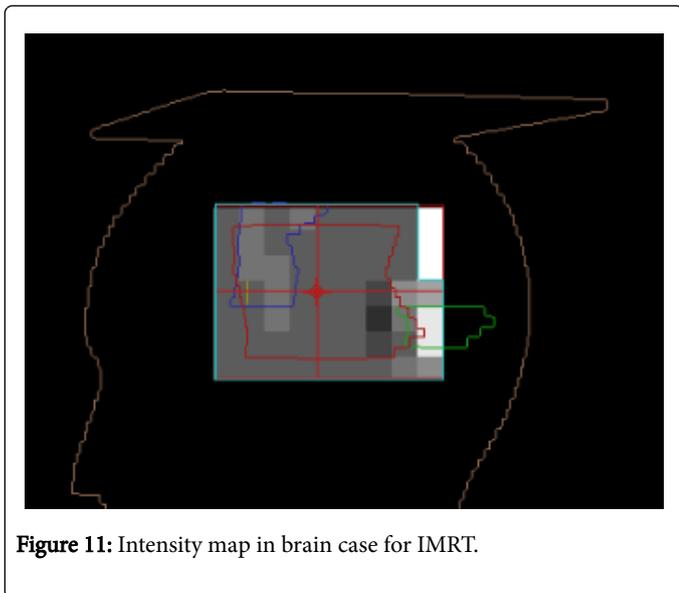**Figure 10:** Beam shape with MLC in brain case for 3DCRT.

Figure 11: Intensity map in brain case for IMRT.

The tumor shape and it's relation with the critical organs is very important in the treatment planning process where the number of treatment fields and its direction will be defined.

IMRT technique increasing the treatment time where the average time for treatment delivery for IMRT cases were 20 minutes. This increase in treatment time was due to the beam splitting to small segments. The average number of the segments were 80 segments per plan. The beam splitting in IMRT increase the MU with significant value and this is showed in Table 1.

Table 2 showed the dosimetric parameters which used as treatment planning evaluation for 3DCRT and IMRT plans.

Case	3DCRT		IMRT	
	No of fields	MU	No of fields	MU
Brain	5 fields	120	5 fields	171
Abdomen	5 fields	116	5 fields	278
Pelvic	5 fields	130	5 fields	342

Table 1: Difference in MU between 3DCRT and IMRT for brain, abdomen and pelvic plan.

Case	3DCRT		IMRT	
	Dose to isocentre	Volume Coverage 95% of dose	Dose to isocentre	Volume Coverage 95% of dose
Brain	100 cGy	100%	100 cGy	100%
Abdomen	100 cGy	100%	100 cGy	99.5%
Pelvic	100 cGy	100%	100 cGy	99%

Table 2: Dose at isocentre and the volume coverage of 95% of dose in 3DCRT and IMRT for Brain, abdomen and Pelvic plan.

For IMRT plans the surface dose were calculated at 4 points in each field size. The points were distributed around the beam isocentre on the axial plan. The depth of the 4 points was 0.07 cm from the outer patient contour. The dose for each point was collected and the average values for the four points were calculated. Using TLD system the dose at these points was measured on the human phantom.

For 3DCRT the surface dose was calculated only at the beam entrance point and compared with that measured at this point during dose delivery.

Surface dose for IMRT technique

Measured and calculated surface doses for 6 MV for brain, abdomen and pelvic cases in IMRT technique were shown in Table 3.

For brain case the surface dose were measured for the 5 beams and compared with the calculated surface dose. TLD ships were seated in the measurement positions during the delivery of the 5 beams to measure the dose component from the whole fields on each point.

As shown in Table 3 the differences between measured (Meas.) and calculated (Calc.) surface dose in brain were -2.82% and the negative sign mean that the measured surface dose were less than the calculated one.

For abdomen as shown in Table 3 the differences between measured and calculated surface dose in abdomen case were -1.7%. The

differences between measured and calculated surface doses are due to the differences in point positions between measurement and calculation, where the calculated dose taken inside the outer contour whereas the measured one taken on the surface outside the outer contour.

For pelvic case as shown in Table 3 the differences between measured and calculated surface dose in pelvic case were -2.98% and the negative sign mean that the measured surface were less than the calculated one.

Case	Brain case		Abdomen case		Pelvic case	
	Meas.	Calc.	Meas.	Calc.	Meas.	Calc.
Field 1	9.94	16.6	12.7	12.4	10.1	18
Field 2	23	22.6	14.9	15.2	23.7	10
Field 3	14.4	16.6	14.8	20	7	18
Field 4	14	15.1	15	17	15.9	20
Field 5	17	18	13	14	6.4	12
Mean surface dose%	15.7	17.8	14.1	15.7	12.6	15.6

Table 3: Measured and calculated surface dose for IMRT technique.

Surface dose for 3DCRT technique

Measured and calculated surface doses for 6 MV for brain, abdomen and pelvic cases in 3DCRT technique were shown in Table 4.

For brain case the surface dose were measured and compared with the calculated surface dose at the beam entrance. The TLD ships were located in the measurement position during the delivery of the 5 beams to measure the scattered component from the whole fields on each point. The differences between measured and calculated surface dose for 3DCRT brain cases were -5.4% as shown in Table 4. The differences between measured and calculated surface dose for 3DCRT abdomen cases were -4.1% and the differences between measured and calculated surface dose for 3DCRT pelvic cases were 3.56% as shown in Table 4.

Case	Brain case		Abdomen case		Pelvic case	
	Meas.	Calc.	Meas.	Calc.	Meas.	Calc.
Field 1	8.83	13.8	14.5	17.6	12.7	14
Field 2	19.58	36	13.5	18.5	12.3	17
Field 3	17.49	29	13.9	18.5	10.7	18.5
Field 4	15	14	14	17	14	18.8
Field 5	17	20	14.5	14	11.7	15
Mean surface dose%	15.3	21.7	13.9	18.2	12.28	16.66

Table 4: Measured and calculated surface dose for 3DCRT technique.

The impact of IMRT on surface doses is very important and needs more investigations and this can be cleared by direct comparison

between the surface doses in IMRT and 3DCRT. Table 5 showed the measured surface doses for 6 MV for brain, abdomen and pelvic cases in 3DCRT and IMRT technique.

Case	IMRT	3DCRT	Differences
Brain	15.78	15.3	0.48
Abdomen	14.13	13.96	0.17
Pelvic	12.62	12.28	0.34

Table 5: Comparison between surface dose in IMRT and 3DCRT.

From Table 5 there were very small differences between surface doses in 3DCRT and IMRT technique. These differences were 0.48% in the brain case, 0.17% in the abdomen case and 0.34% in pelvic case.

Discussion

The increase in surface dose with increasing field size is due to increased electron emission from the collimator and air, Photons back scattered from the patient and high energy electrons produced by photon interactions in air and any Shielding structures in the vicinity of the patient.

The results showed a significant increase of surface dose with increasing the gantry angle oblique incidence. The relation between surface dose and the gantry angle can be explained by the concept of electron range surface (ESR) Jackson et al. (Figure 12) [10]. The ERS is a 3-D representation of secondary electron range and distribution produced by a pencil beam of photons interacting with the medium. Electrons generated inside the ERS volume will reach the point P and contribute to the dose there, where as those generated outside, because of their inadequate range, make no contribution. The ERS for 60Co γ rays is in the shape of an ellipsoid with axial dimensions emissions of 5 × 2.4 mm.

They reported that the increase in the angle of incidence of the photon beam results in additional surface dose at P because of electron contribution from the portion of the ERS, which appears below the plastic water phantom surface (hatched curve). For tangential beam incidence, since half of the ERS is below the plastic water phantom surface. Another important effect associated with oblique angles is that as the surface dose increases with the angle of incidence, the depth of maximum build-up decreases. The dose reaches its maximum value faster at glancing angles than at normal incidence. As a result, the dose build-up region is compressed into a more superficial region. Under these conditions, a high skin reaction becomes much more likely.

Build-up region dose decreases for IMRT fields compared to conformal therapy fields for 6MV, but the general effect is mild (~10%). The dominant characteristics are the addition of dose due to MLC transmission contributing to useful dose while decreasing primary beam exposure and the increase in blocking of the contamination radiation emanating from the treatment head. Since the transmission field is more penetrating for 6MV and the collimator leaves potentially screen a portion of the contaminating radiation, the surface build-up dose experiences a relative decline [11].

Skin dose depends on electron contamination primarily from the photon interactions in the build-up region which increase with field size and secondarily from air and collimation systems. Oblique incidence of the treatment fields increase the electron contamination

and this is can explain the surface dose equivalent between IMRT and 3DCRT.
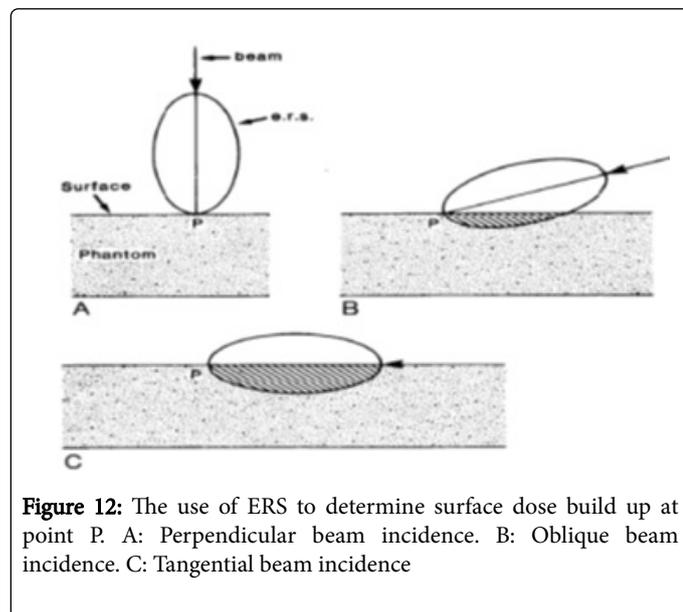

Figure 12: The use of ERS to determine surface dose build up at point P. A: Perpendicular beam incidence. B: Oblique beam incidence. C: Tangential beam incidence

The build-up dose near the surface is highest for the open field and lowest for the smallest strip field. The use of an individual IMRT field does not significantly increase the skin dose above that of a conventional photon field [12]. For a 12 × 12 cm field size, surface dose (at 0.07 cm) measured by advanced Markus chamber is 19.8% for open field and 19.2% for an un-modulated step-and-shoot IMRT field [13]. The addition of MLC transmission dose to the treated field has the effect of lowering the build-up region dose because the transmitted radiation is more penetrating (hardened) than the original beam for 6MV photons [14,15].

Conclusions

The chosen planning and optimization strategy can affect skin dose specially including skin as a sensitive structure. Knowing the skin dose leads to prediction of skin reactions and helping with designing new treatment techniques. Surface dose increased with decreasing energy so low energy could be used for tumor near surface. Surface dose depends strongly on field size and obliquity of the gantry so surface dose can be decreased by using direct incidence of the beam and decreasing field size as possible to avoid skin reaction.

Differences between measured and calculated doses can be used in making calibration of TPS. A factor can be taken depending on field size. Parallel plate ion chamber is more accurate than TLD in measuring surface dose so a correction factor can be taken. Percentage surface dose don't change with different SSD or SAD. Differences between fields with and without tissue equivalent material were stable so we can take the dose factor for 1 cm wax block independent of field size. By using block tray surface dose increased with increasing field size specially for large field sizes so we can use Perspex tray in whole body irradiation cases. Surface dose in IMRT technique was slightly higher than that in 3DCRT.

The differences between measured and calculated surface dose at depth 2 mm were less than differences at surface. This means that TPS is more accurate with increasing depth. For irregular tumor shape and closed OAR the IMRT is a good solution to cover the tumor and spare the critical organs without increasing the skin dose.

References

1. Nadir K, Ayhan K, Gönül K, Lütfi Ö, Kayhan E (2002) Analyses of surface dose from high energy photon beams for different clinical setup parameters. Turk J Med Sci 32:211-215.
2. (1997) The use of plane parallel ionization chambers in high energy electron and photon beams,"IAEA Technical report 381, IAEA, Vienna.
3. (1975) ICRP Publication 23, Anatomical, Physiological and Metabolic Charac- teristics Pergamon, Oxford.
4. (1978) ICRP Publication 28, The Principles and General Procedures for Han- dling Emergency and Accidental Exposures of Workers Pergamon, Oxford.
5. (1991) ICRP Publication 60, Recommendations of the International Commission on Radiological Protection, Pergamon, Oxford,.
6. (1985) Determination of dose equivalents resulting from external radiation sources (Report No. 39) International Commission on Radiation Units and Measurement, Washington, DC.
7. Girigesh Yadav, RS Yadav, Alok Kumar (2009) Skin dose estimation for various beam modifiers and source-to-surface distances for 6MV photons. J Med Phys 34:87-92.
8. Bilage H, Ozbek N, Okutan N, Cakir A, Acar H (2010) Surface dose and build-up region measurements with wedge filters for 6 and 18 MV photon beams. Jpn J Radiol 28:110-116.
9. Kim S, Liu CR, Zhu TC, Palta JR (1998) Photon beam skin dose analyses for different clinical setups. Med Phys 25:860-866.
10. Jackson W (1971) Surface effects of high-energy x-rays at oblique incidence. Br J Radiol 44:895-896.
11. Yokoyama S, Roberson PL, Litzenberg DW, Moran JM, Fraass BA (2004) Surface buildup dose dependence on photon field delivery technique for IMRT. J Appl Clin Med Phys 5:71-81.
12. S Price, M Williams, M Butson, P Metcalfe (2006) Comparison of skin dose between conventional radiotherapy and IMRT. Australas Phys Eng Sci Med 29:272-277.
13. FQ Chen, R Gupta, P (2010) Metcalfe Intensity modulated radiation therapy (IMRT) surface dose measurements using a PTW advanced Markus chamber. Australas Phys Eng Sci Med 33:23-34.
14. Khan FM (1994) The physics of radiation therapy, Williams and Wilkin, Baltimore. 323-332.
15. Court LE, Tishler R, Xiang H, Allen AM, Makrigiorgos M, et al. (2008) Experimental evaluation of the accuracy of skin dose calculation for a commercial treatment planning system. J Appl Clin Med Phys 9:2792.